1 **Special Article:**

2 **Explaining patterns of avian diversity and endemicity:**

3 **climate and biomes of southern Africa over the last 140,000 years**

4 Brian Huntley[1]*, Yvonne C. Collingham[1], Joy S. Singarayer[2], Paul J. Valdes[3],

5 Phoebe Barnard[4,5,6], Guy F. Midgley[7], Res Altwegg[6,8] and Ralf Ohlemüller[9]

6 [1] School of Biological and Biomedical Sciences, Durham University, South Road, Durham DH1 3LE,

7 United Kingdom

8 [2] Department of Meteorology and Centre for Past Climate Change, University of Reading, Earley Gate,

9 PO Box 243, Reading RG6 6BB, United Kingdom

10 [3] School of Geographical Sciences, University of Bristol, University Road, Bristol BS8 1SS,

11 United Kingdom

12 [4] Climate Change BioAdaptation, South African National Biodiversity Institute, Kirstenbosch Research

13 Centre, P/Bag X7, Claremont 7735, Cape Town, South Africa

14 [5] Percy FitzPatrick Institute of African Ornithology, DST-NRF Centre of Excellence,

15 University of Cape Town, Rondebosch 7701, Cape Town, South Africa

16 [6] African Climate and Development Initiative, University of Cape Town, Rondebosch 7701,

17 Cape Town, South Africa

18 [7] Department. of Botany and Zoology, Stellenbosch University, Private Bag X1, Matieland 7602,

19 South Africa

20 [8] Statistics in Ecology, Environment and Conservation, Department of Statistical Sciences, University of

21 Cape Town, Rondebosch 7701, Cape Town, South Africa

22 [9] Department of Geography, Richardson Building, University of Otago, PO Box 56, Dunedin,

23 New Zealand

24 * **Corresponding author:** Prof Brian Huntley

25   School of Biological and Biomedical Sciences

26   Durham University

27   South Road

28   Durham   DH1 3LE

29   United Kingdom

30   brian.huntley@durham.ac.uk

31 **Running heading:** Explaining avian diversity and endemicity patterns

Abstract

Aim: Test hypotheses that present biodiversity and endemic species richness are related to climatic stability and/or biome persistence.

Location: Africa south of 15° S.

Methods: Seventy eight HadCM3 general circulation model palaeoclimate experiments spanning the last 140,000 years, plus a pre-industrial experiment, were used to calculate measures of climatic variability for 0·5° grid cells. Models were fitted relating distributions of the nine biomes of South Africa, Lesotho and Swaziland to present climate. These models were used to simulate potential past biome distribution and extent for the 78 palaeoclimate experiments, and three measures of biome persistence. Climatic response surfaces were fitted for 690 bird species regularly breeding in the region and used to simulate present species richness for cells of the 0·5° grid. Species richness was evaluated for residents, mobile species (nomadic or partially/altitudinally migrant within the region), and intra-African migrants, and also separately for endemic/near-endemic (hereafter 'endemic') species as a whole and those associated with each biome. Our hypotheses were tested by analysing correlations between species richness and climatic variability or biome persistence.

Results: The magnitude of climatic variability showed clear spatial patterns. Marked changes in biome distributions and extents were projected, although limited areas of persistence were projected for some biomes. Overall species richness was not correlated with climatic variability, although richness of mobile species showed a weak negative correlation. Endemic species richness was significantly negatively correlated with climatic variability. Strongest correlations, however, were positive correlations between biome persistence and richness of endemics associated with individual biomes.

Main Conclusions: Low climatic variability, and especially a degree of stability enabling biome persistence, is strongly correlated with species richness of birds endemic to southern Africa. This probably principally reflects reduced extinction risk for these species where the biome to which they are adapted persisted.

Keywords: atmosphere–ocean general circulation model; biome persistence; birds; Cape Floristic Region; climatic stability; Heinrich Events; last glacial–interglacial cycle; species richness.

INTRODUCTION

Global climatic conditions varied substantially during the late Quaternary, extended glacial and short interglacial stages alternating during the last 800–1000 kyr (EPICA community members, 2004). The last 140 kyr spans the final millennia of the penultimate glacial, last interglacial, last glacial and post-glacial (Holocene). Climatic conditions globally were mostly markedly colder than the recent past, although somewhat warmer for part of the last interglacial and to a lesser extent the early Holocene. The last glacial stage also had large millennial climatic fluctuations (Bond *et al.*, 1997; Wolff *et al.*, 2010).

Palaeoecological evidence shows that species responded to these climatic changes mainly by changing their distribution and/or abundance at regional to continental scales (McGlone, 1988; Huntley & Webb, 1989; Graham & Grimm, 1990; Huntley, 1991; Markgraf, 1993; Markgraf & McGlone, 2005; Marchant *et al.*, 2009). Many species' populations were at times severely reduced as species were extirpated from previously occupied areas, not only in glaciated North America and Europe (Ehlers & Gibbard, 2004), but wherever climatic changes made conditions unsuitable for species' persistence. These extirpations often markedly reduced the extent and/or spatial continuity of species' distributions, with consequent population isolation and overall population decreases. In turn, population bottlenecks resulted in loss of genetic diversity (MacPhee *et al.*, 2005; Campos *et al.*, 2010), probably contributing to extinction of some species, whilst increased isolation of sub-populations led to genetic differentiation (Hewitt, 1996, 2001) and probably speciation.

Southern Africa (10 – 35°E, 15 – 40°S; Fig. 1) includes the Greater Cape Floristic Region (Allsopp *et al.*, 2014), an area of globally high diversity and endemicity, especially amongst higher plants but also other taxa, including birds (Colville *et al.*, 2014). Even in such unglaciated or minimally glaciated regions (Boelhouwers & Meiklejohn, 2002; Mills *et al.*, 2012), climatic conditions varied substantially over the last glacial–interglacial cycle (Meadows & Baxter, 1999; Partridge *et al.*, 1999; Chase & Meadows, 2007). However, such areas might have high biodiversity because late-Quaternary climatic changes were less than elsewhere, leading to greater persistence of species (Dynesius & Jansson, 2000). Testing this hypothesis requires quantification of the magnitude of late-Quaternary climatic changes and of their relationships with present diversity patterns. Given that species were more likely to be extirpated from more changeable regions, we expect present biodiversity patterns, especially endemic species richness, to reflect patterns in the magnitude of past climatic changes (Huntley *et al.*, 2014). Further, we expect this to

4

94 be more pronounced for species associated with particular biomes, especially biomes that experienced

95 marked late-Quaternary changes in location and/or extent.

96 We aim to test two related hypotheses:

97   1. That present biodiversity, especially endemic species richness, is greater where the late-Quaternary
98   climate was less variable.
99   2. That species richness, especially of biome-associated endemics, is greatest where late-Quaternary
100   climate, although variable, allowed persistence of that biome.

101 **MATERIALS AND METHODS**

102 **Study area**

103 The overall area examined, referred to below as southern Africa, is the land area between 15°S and 40°S

104 and between 10°E and 35°E (Fig. 1).   Climatic variability is assessed for this entire region, and model

105 projections of past biome extents and of avian species richness are also made for the entire region.   The

106 data used to fit models relating biomes to climate extend over only South Africa, Lesotho and Swaziland

107 (Figure S1 in Appendix S1), whilst the data used to fit models relating bird species' reporting rates to

108 climate extend over these countries and also over Namibia, Botswana and Zimbabwe.

109 **Palaeoclimatic changes**

110 Results from 78 palaeoclimate experiments and a pre-industrial experiment using a consistent configuration

111 of the Hadley Centre unified model (Singarayer & Valdes, 2010), a fully-coupled atmosphere–ocean

112 general circulation model (AOGCM) including interactive sea-ice (Gordon *et al.*, 2000), were used to derive

113 regional palaeoclimatic estimates.   Experiments were performed for time slices from 140 ka to 1 ka at

114 intervals of 1 kyr (1 – 22 ka), 2 kyr (24 – 80 ka and 120 – 140 ka) or 4 kyr (84 – 116 ka);   seven 'hosing'

115 experiments designed to mimic Heinrich Events H0 – H6 (13, 17, 24, 32, 38, 46 and 60 ka) were also

116 performed.   Singarayer and Valdes (2010) provide details of model configuration and derivation of

117 boundary conditions and forcings applied.

118 For each palaeoclimate experiment, anomalies were computed relative to the pre-industrial experiment for

119 monthly mean temperature, precipitation and cloudiness.   Thin-plate splines were fitted to these anomalies

120 at GCM grid cell resolution (2·5° latitude x 3·75° longitude) and used to interpolate them to a 0·5°

longitude x latitude grid (using ANUSPLIN, Hutchinson, 1989). Regional palaeoclimate scenarios were obtained by applying interpolated anomalies to observed recent (1961–90) values from the Climatic Research Unit 0·5° dataset (CRU CL 1.0, New *et al.*, 1999). A modified version of the FORTRAN program BIOCLI (Wolfgang Cramer and Rik Leemans) was used to calculate nine bioclimatic variables for each grid cell and palaeoclimate scenario: annual thermal sums above 0°C (GDD0) and 5°C (GDD5); mean temperatures of the coldest (MTCO) and warmest (MTWA) months; an estimate of the annual ratio of actual to potential evapotranspiration (AET/PET); annual total intensity of the wet (TOTWETINT) and dry (TOTDRYINT) season(s); and maximum wet (MAXWETINT) and dry (MAXDRYINT) season intensity (see Huntley *et al.*, 2006 for details). Each grid cell was assigned to one of three seasonal rainfall zones for each scenario (Appendix S2) and the frequency with which it was assigned to each zone counted.

Values for each bioclimatic variable were standardized to zero mean and unit standard deviation across all grid cells and time slices; standardized values were used to calculate Euclidean distances for each grid cell between climatic conditions for each time slice, including 1961–90 (hereafter 'present'), and every other time slice. Three measures of climatic variability of each grid cell were then computed: maximum; mean; and standard deviation of Euclidean distances. Each was calculated for Euclidean distances between present climate and the 78 palaeoclimates, hereafter 'variability relative to present', and between the climate of each time slice and that of every other, hereafter 'overall variability'. Calculations were performed using purpose-written FORTRAN programs. Climatic variability measures were mapped to reveal any spatial patterns (using ArcGIS® and CorelDraw X6®). The frequency with which maximum Euclidean distance corresponded to each time-slice pair was counted across all grid cells.

Changes in biome extent and location

Quantitative climatic response surfaces (Huntley *et al.*, 2012) were fitted to model relationships between the extents and locations of nine biomes mapped for South Africa, Lesotho and Swaziland by Mucina and Rutherford (2006, see Fig. S1 in Appendix S2) and present climate. Extent of each biome in each 0·5° grid cell was expressed as a proportion of that grid cell's land area falling within South Africa, Lesotho and/or Swaziland. Two models were fitted for each biome, each using four bioclimatic variables. All models included MTCO, MTWA and AET/PET, the fourth variable being either TOTWETINT or TOTDRYINT; these variables were selected on the basis of known mechanisms through which they influence vegetation character. Model performance was assessed using the correlation between the

150 proportion of each grid cell's land area mapped as occupied, and predicted by the model to be occupied

151 under present climatic conditions, by the biome.   The model for each biome giving the higher correlation

152 was used to project its potential distribution for the entire region of southern Africa for each palaeoclimate

153 scenario.   The validity of such a spatial extrapolation of the models was assessed by comparing the

154 biomes simulated for the present climate with observations of the current distribution of biomes.   Models

155 were fitted and their performance assessed using custom-written FORTRAN programs (based partly on

156 programs written by Patrick J. Bartlein, see Huntley *et al.*, 1989).

157 Potential total extent of each biome in southern Africa for each time slice was computed by summing

158 simulated proportions across grid cells, then normalizing values for each time slice to a sum across biomes

159 equal to the total number of grid cells (1461).   Minimum, maximum and mean potential total extent of each

160 biome were computed as absolute values and as percentages of its simulated present extent.

161 Potential past biome patterns were mapped by assigning each grid cell to the biome simulated to dominate

162 that cell for that time slice, the dominant biome being that simulated to occupy the maximum extent.   The

163 number of grid cells dominated by each biome was also counted for each time slice.   Three measures of

164 persistence of each biome were computed for each grid cell across all time slices: (i) the frequency with

165 which the cell was simulated to have been dominated by the biome;   (ii) the mean percentage of the cell

166 simulated to have been occupied by the biome;   and (iii) the frequency with which the biome was

167 simulated to have been present in the cell, presence being assigned when simulated biome extent in the

168 cell exceeded the threshold value that maximised qualitative goodness-of-fit of its response surface model

169 as assessed using the true skill statistic (Allouche *et al.*, 2006).   Frequencies were mapped to reveal any

170 cell(s) where a biome was consistently potentially present or dominant.

171 **Present avian diversity patterns**

172 Bird distribution data were obtained from the Southern African Bird Atlas Project (SABAP, Harrison *et al.*,

173 1997) at 0·25° resolution for South Africa, Lesotho, Swaziland, Namibia and Zimbabwe, and at 0·5°

174 resolution for Botswana.   These data record species' reporting rates, i.e. proportion of cards returned for a

175 grid cell on which the species was recorded.   Quantitative response surface models relating species'

176 reporting rates to present climate were fitted as described by Huntley *et al.* (2012), using four bioclimatic

variables (MTCO, MTWA, AET/PET and TOTDRYINT) shown previously most often to give the best-fitting model (Huntley *et al.*, 2012).

We fitted models for 697 species regularly breeding in the region, categorised by Hockey *et al.* (2005) as residents (207 spp.), altitudinal or partial migrants or nomadic (hereafter 'mobile species', 402 spp.), or intra-African migrants (88 spp.). Long-distance, mainly inter-continental, migrants were excluded because their richness patterns are unlikely to reflect longer-term stability of regional climate and/or biomes; vagrants were excluded because their occurrences are sporadic. Species endemic or near-endemic to southern Africa (hereafter 'endemics') were distinguished from more widespread species, and endemics were categorised according to the biome(s) predominantly used (following Hockey *et al.*, 2005).

Models successfully fitted for 690 species were used to simulate each species' potential present reporting rate for each 0·5° cell of the entire study region. This required spatial extrapolation of the models beyond the region from which data were available for model fitting, albeit to a much more modest extent than in the case of the biome models. Rather than reduce these reporting rates to presence–absence and count presences, we summed simulated reporting rates for a cell to obtain a measure of its potential species richness. Sums were calculated for: (i) all species; (ii) all residents (203); (iii) all mobile species (399); (iv) all intra-African migrants (88); (v) all widespread (i.e. non-endemic) species (524); (vi) all endemics (163; two intra-African migrants categorised by Hockey *et al.* (2005) as near-endemic and one as an endemic breeder, respectively, were excluded); (vii) endemic residents (53); and (viii) endemic mobile species (108). Relationships between contemporary species richness and past climatic variability were assessed using the Pearson product–moment correlation coefficient. Species richness of endemics associated with each biome was also computed for each cell. It was necessary to combine Succulent Karoo and Nama Karoo for this analysis as they are not distinguished by Hockey *et al.* (2005) when indicating principal habitats used by bird species. In addition, no analysis could be performed for the Indian Ocean Coastal Belt as this is not distinguished by Hockey *et al.* (2005) as a potential habitat. Relationships between contemporary species richness and biome persistence were again assessed using the Pearson correlation coefficient. In this case correlations were calculated both for all 1461 grid cells in the study area and for 823 grid cells south of 22°S, the northernmost latitude to which data used to fit response surface models for the biomes extended.

RESULTS

Palaeoclimatic changes

Considering maximum climatic differences relative to present (Fig. 2(a)), lowest variability was principally in an area corresponding to the present extent of the Nama Karoo and Fynbos biomes (Fig. S1 in Appendix S1), with outlying relatively stable grid cells along the southern half of the west coast and in a broad area in the east. Greatest variability was principally in the north-west, especially centred upon the area of stabilized dunes lying between the Etosha Pan and Okavango Delta and extending north across the Caprivi Strip to span the borders of Namibia, Angola and Botswana (Thomas *et al.*, 2000). Overall variability maxima show a similar pattern (Fig. 2(d)), though with a more marked area of low variability extending from south-eastern Namibia to the centre of the Western Cape province of South Africa. Greatest variability was again mainly in the north-west and the stabilised dune-field. Considering grid cells simulated to be dominated by each biome under present climate, medians and third quartiles for maximum overall Euclidean distance were smaller for those of the Indian Ocean Coastal Belt, Nama Karoo, Fynbos and Succulent Karoo (Table S3 & Fig. S2 in Appendix S3). Climate over the past 140 kyr is thus simulated to have been more stable in areas currently occupied by these biomes than in areas occupied by the remaining biomes, although a minority of grid cells in the Nama Karoo show greater variability. This area of relative climatic stability broadly corresponds to the year-round rainfall zone both at present and most persistently over the past 140 kyr (Figs. S7 & S8 in Appendix S3).

Across the 1461 grid cells, maximum differences from present climate were for a Heinrich Event stadial in 1288 cases, with maximum difference for almost 23% of grid cells being with respect to H2 (H0 61; H1 221; H2 331; H3 143; H4 47; H5 259; H6 226). When all pairwise comparisons were examined, 124 ka contributed to the maximum pairwise difference in 959 cases, the other partner in most cases (942) being a Heinrich Event, with H2 again the most frequent (H0 14; H1 244; H2 383; H3 48; H4 30; H5 190; H6 33). Other pairs giving maximum difference for >20 grid squares all included a Heinrich Event; they were: H0 *vs* 19 ka (21); H0 *vs* 22 ka (143); 16 ka *vs* H5 (23); 17 ka *vs* H5 (21); 19 ka *vs* H6 (87); 22 ka *vs* H5 (48); 28 ka *vs* H6 (48); and H6 *vs* 120 ka (21). Overall, a Heinrich Event was one of the pair giving maximum difference in >98% of cases (1433 of 1461 grid cells).

Mean Euclidean distances with respect to present climate and overall (Figs. 2(b) & (e)) show strikingly different spatial patterns. They also show, especially for mean differences from present climate, a pattern distinctly different from that for maximum differences (Fig. 2(a)). Lowest variability with respect to present (Fig. 2(b)), is focused in the west of Northern Cape province and southern Namibia, the most stable area being on the coast of south-west Namibia. For overall variability (Fig. 2(e)) the pattern is similar to that for maximum differences (Figs. 2(a) & (d)), with a broad area of relatively low variability extending from south-eastern Namibia south to central Western Cape, albeit with relative stability in coastal areas with low mean differences from present climate (Fig. 2(b)), and greatest variability in north-west Namibia/south-west Angola and the stabilised dunes spanning the Namibia, Angola and Botswana borders.

The patterns for standard deviation of Euclidean distances (Figs. 2(c) & (f)) again differ somewhat between variability with respect to present climate and overall variability. Both show areas of lowest variability centred in the Western Cape and in south-east Namibia. There is also a more limited area of low variability along the coast of north-east Eastern Cape province and south-west Kwazulu-Natal. For variability with respect to present climate, a much more extensive area of low variability extends from the east of Eastern Cape through Kwazulu-Natal to southern Mozambique. In both cases variability is generally lower in South Africa than in areas to the north, with greatest variability corresponding mainly to areas of greatest variability as assessed by both mean and maximum Euclidean distances.

Changes in biome extent and location

Response surface models for biomes all gave high correlations with observed data when used to simulate biome extents in the 0·5° grid cells of South Africa, Lesotho and Swaziland for present climate (Table S1 in Appendix S1). The model using TOTWETINT gave a higher correlation for Desert, Fynbos and Forest, the TOTDRYINT model performing better for the other biomes. The better performing models for individual biomes had correlations of between 0·901 (Forest) and 0·969 (Indian Ocean Coastal Belt). Relatively poor model performance for Forest is because this biome accounts for <0·4% of the land area and does not dominate any grid cells. The simulation of present biomes for the entire study region broadly accorded with observed and simulated regional biome patterns (see e.g. Scheiter & Higgins, 2009), no substantially different biomes occurring in the region.

259   Aside from revealing a general dynamism of biome distributions since 140 ka, maps of dominant biomes

260   (Fig. 3) reveal several systematic patterns.   Visually the most striking are the large and complementary

261   changes in extent of Nama Karoo and Grassland, and the simulated extensive presence of Fynbos in the

262   north of the region and markedly increased simulated extent of Succulent Karoo under many palaeoclimate

263   scenarios.   When plotted against age (Fig. 4), the relative extent of most biomes is clearly related to

264   austral summer insolation at 30°S, and also responds markedly to climatic conditions simulated for Heinrich

265   Events.   The relative extent of Savanna more closely mirrors global climatic signals such as $[CO_2]_{atm}$ and

266   the $\delta^{18}O$ record from Greenland (Fig. S4 in Appendix S3).   Evidence of core areas of persistence of

267   several biomes is seen when the frequency with which each dominates grid cells is mapped (Fig. 5).

268   Accounts of the simulated history of each biome are provided in Appendix S2 and details of the simulations

269   given in Appendix S3 (Tables S4, S5 and S6, Fig. S3).

270   **Relationships of present avian diversity to climatic variability**

271   Response surface models fitted for 690 southern African bird species were good, with a high median

272   correlation between observed and simulated reporting rates of 0·585 ($n = 3964$, $p << 0.001$).   The

273   performance for endemics was better than that for widespread species, with median correlations of 0·630

274   *vs* 0·560;   this is expected given that virtually all of the geographical, and hence climatic, range of the

275   former is encompassed by the data used to fit the models.   Qualitatively the models also performed well,

276   with median true skill statistic (Allouche *et al.*, 2006) for all (endemic *vs* widespread) species of 0·842

277   (0·855   *vs* 0·835) and median Cohen's kappa (Cohen, 1960) of 0·720 (0·753 *vs* 0·710).

278   Endemic species richness patterns differed from those of species as a whole;   species of different

279   movement categories also showed different patterns (Appendix S2;   Figs. S5 & S6 in Appendix S3).

280   When considering all species, more than half the correlations between species richness and climatic

281   variability are positive, although mostly of small magnitude (Table 1).   Strongly positive correlations

282   indicate greater species richness overall, as well as of residents and intra-African migrants, where mean

283   difference from present climate has been higher over the last 140 kyr.   Two strongly negative correlations

284   relate to mobile species, indicating that these species achieve greater richness where standard deviations

285   of climatic differences are lower.   Mobile species richness thus tends to accord with expectation, being

286   greater where climatic variability (assessed by standard deviations of Euclidean Distances) has been less.

287   Correlations for widespread species are all positive, indicating that their species richness tends to be

288   greater where climate has been more variable.   In contrast, correlations for endemics not only all have the

289   expected negative sign, but are also on average 3·36 x greater in absolute values than correlations for

290   species as a whole, all achieving high significance (Table 1).   For endemics as a whole, and for endemic

291   mobile species, highest correlations are with mean climatic differences from present, whereas for endemic

292   resident species highest correlation is with standard deviation of overall climatic differences.   Current

293   species richness patterns of endemics thus accord with expectation, with higher species richness where

294   climate has been less variable over the last glacial–interglacial cycle.

295   **Relationships of present avian diversity to biome persistence**

296   The alternative measures of biome persistence showed broadly similar spatial patterns (Fig. 5, Fig. S3 in

297   Appendix S3).   All biomes except Forest were persistently present across all 79 time slices in at least a

298   small number of grid cells, whereas only four biomes (Succulent Karoo, Fynbos, Grassland and Savanna)

299   persistently dominated one or more grid cells. Correlations between the first measure of biome

300   persistence and avian diversity could not be calculated for Forest associated species because this biome

301   never dominated any grid cells.   Simulated patterns of species richness for endemics associated with each

302   biome showed the expected general spatial patterns (Fig. S6 in Appendix S3).   However, because many

303   species are not restricted to a single biome, areas with lower numbers of biome-associated species are

304   much more extensive than the area of occurrence of that biome.

305   For six of the biomes that could be analysed, all correlations between biome persistence and avian

306   diversity were, as expected, strongly positive (Table 2).   Strongest correlations were for Grassland, Karoo

307   and Desert, with lower values for Forest, Fynbos and Albany Thicket.   Highest correlations for Karoo and

308   Desert were with their frequency of occurrence across the study area as a whole, whilst for Forest the

309   highest correlation was with its frequency of occurrence south of 22°S.   For Grassland, Fynbos and

310   Albany Thicket highest correlations were with their mean percentage occupied south of 22°S, Fynbos, as

311   expected, showing the strongest increase in correlations when analysis was constrained to the southern

312   part of the study area because this excludes those areas in the north often simulated as occupied by

313   Fynbos (Fig. 3), but remote from the area simulated as consistently dominated by this biome (Fig. 5(d)) and

314   also consistently disjunct from the latter area.

315 Thus for these six biomes the evidence strongly supports our second hypothesis, that present species

316 richness of biome-associated endemics is highly correlated with degree of persistence of the biome in that

317 grid cell during the last glacial–interglacial cycle.

318 Savanna was the exception to this pattern. For the study area as a whole correlations were significant

319 and negative; correlations for the area south of 22°S, although positive, were weak. Simulated

320 persistence of Savanna was greatest in the north and east (Fig. 5(g), Fig. S3(g) in Appendix S3), whereas

321 the area richest in savanna-associated regional endemics lies mostly south of 22°S and centrally in terms

322 of longitude (Fig. S6(g) in Appendix S3), overlapping only to a limited extent with areas of high persistence

323 of the biome.

324 **DISCUSSION**

325 Previous studies have advanced a wide range of hypotheses to account for global and/or regional patterns

326 of biodiversity and/or of endemism (see e.g. Dynesius & Jansson, 2000; Gaston, 2000). These

327 hypotheses can broadly be categorised into those that explain patterns in terms of present environment

328 versus historical factors. Present patterns of productivity, climate and topographic diversity all correlate

329 with biodiversity patterns in at least some regions (Rahbek & Graves, 2001; Jetz & Rahbek, 2002; Thuiller

330 *et al.*, 2006), but present environment attributes alone cannot generally account for present biodiversity

331 patterns (Jetz *et al.*, 2004). Historical factors, in contrast, can often account for these patterns more

332 completely (Huntley, 1993; Araújo *et al.*, 2008; Voelker *et al.*, 2010; Sandel *et al.*, 2011; Huntley *et al.*,

333 2014). Historical factors may operate over a range of time scales, from millions of years (e.g. Linder &

334 Hardy, 2004; Voelker *et al.*, 2010) through the multi-millennial glacial–interglacial cycles of the Quaternary

335 (e.g. Huntley, 1993; Dynesius & Jansson, 2000) to the millennial climatic fluctuations of the last glacial

336 stage (Huntley *et al.*, 2014).

337 We focus upon the most recent glacial–interglacial cycle, including millennial fluctuations characteristic of

338 glacial stages, and test two alternative hypotheses to account for present patterns of avian species

339 richness in southern Africa: (i) present biodiversity, especially endemic species richness, is greater where

340 late-Quaternary climate was less variable; and (ii) species richness, especially of biome-associated

341 endemics, is greatest where late-Quaternary climate, although variable, allowed persistence of that biome.

342 Unfortunately the generally sparse independent evidence of past climates and biomes in the region, prior to

343 the Holocene (Chase & Meadows, 2007), severely limits assessment of the extent to which simulated

344 palaeoclimate and biome patterns accord with observations.   There is neither a sufficiently dense spatial

345 coverage of such evidence, nor sufficient independently-dated or stratigraphically continuous evidence for

346 the last glacial stage and last interglacial, to support systematic assessment of our modelling results.

347 Furthermore, as Huntley *et al.* (2014) discussed, at least some of the palaeoclimatic evidence is

348 contradictory.   Nonetheless, the AOGCM results are in overall agreement with those few records that are

349 available, with some striking examples of detailed agreement (Huntley *et al.*, 2014; Singarayer & Burrough,

350 2015).   Comparison of the palaeoclimate simulation results with data from marine sediment cores

351 collected in the adjacent oceans (e.g. Kim *et al.*, 2003) supports this conclusion.   Similarly, when

352 expressed in terms of seasonal rainfall patterns, there is broad agreement between the palaeoclimate

353 scenarios (Appendix S2, Figs. S7–9 in Appendix S3) and palaeoenvironmental evidence (Chase &

354 Meadows, 2007).

355 Although we modelled only the influence of past climate on biome distribution, well-documented glacial–

356 interglacial changes in atmospheric carbon dioxide concentration ($[CO_2]_{atm}$) (e.g. Petit *et al.*, 1999) would

357 have shifted the competitive balances between woody and herbaceous plants (Bond & Midgley, 2012), and

358 between C3 and C4 species (Polley *et al.*, 1993).   This probably most directly affected the distribution of

359 the savanna biome that is defined by the relative dominance of grasses versus trees.   Our models

360 probably over-predict the spatial extent of savanna and under-predict that of grassland when $[CO_2]_{atm}$ was

361 lower during glacial stages.   We explore here only the role of climate, however, because sufficiently

362 credible dynamic vegetation models incorporating plant growth forms and disturbance regimes needed to

363 investigate the interacting effects of changes in climate and $[CO_2]_{atm}$ are not yet available.   Whilst progress

364 is being made, more work is required both on representing tree–grass interactions and resulting biome

365 structure under varying $[CO_2]_{atm}$, and especially on developing representations of shrub and succulent

366 growth forms that dominate some southern African biomes.

367 Difficulties in validating our simulations of palaeoclimates and limitations of our approach to modelling past

368 biome distributions notwithstanding, their reliability is supported by our results (Tables 1 & 2).   No

369 consistent pattern emerged with respect to relationships between overall species richness (widespread *plus*

370 endemic species) and climatic stability.   Fewer than half of the correlations had the expected sign, and

14

only two with the expected sign achieved high significance (Table 1). However, the patterns for endemics were clear and consistent with both our hypotheses. Species richness of endemics was generally higher in areas with less variable climate over the past 140,000 years (Table 1). We did not expect weaker correlations for endemic resident species than for all endemics or for mobile endemics. However, a relatively higher proportion of resident than mobile endemics occurs in the Savanna biome than in other biomes (compare Fig. S5(e) & (f) in Appendix S3). The correlation of Savanna-associated endemic richness with biome persistence is also weaker than for other biomes (Table 2). Savanna, however, is likely to have responded more than other biomes to the lowered $[CO_2]_{atm}$ during the glacial, with resulting greater equatorward contraction meaning it was likely to have been extensive mainly north of our study region at the last glacial maximum (Elenga *et al.*, 2000). This greater sensitivity and equatorward contraction would offer scope for, and favour adaptation of, regional Savanna-associated endemics to track biome shifts. Similarly, past range shifts and/or northward contractions likely account also for the lack of the expected relationship in the case of widespread species. Indeed evidence of higher present richness in more climatically variable areas is consistent with such a response. Among mobile species as a whole the relationship between richness and climatic stability is generally weaker. This may indicate that such partial and altitudinal migrants, and nomads, persisted by making local movements, paralleling their responses to seasonal and inter-annual climatic variability and exploiting the opportunities offered by topographically diverse landscapes. Such contrasting responses to climatic change pose challenges for biodiversity conservation.

There were generally stronger correlations between biome persistence and richness of biome-associated endemics (Table 2). This indicates that it is not primarily the absolute magnitude of climatic variability that leads to reduced current richness of endemics, but the extent to which climatic conditions have changed sufficiently to result in biome replacement. Persistence of a biome in a given geographical location is likely to reduce extinction risk amongst biome-associated endemics, whereas biome replacement will frequently cause local extinction. If extensive and repeated over time, this will likely reduce the overall number of endemics associated with the biome. Furthermore, a combination of biome persistence and moderate climatic variability may favour the evolution of new biome-associated endemics (Midgley *et al.*, 2005). Whilst our results for birds will not necessarily apply also to other taxonomic groups in southern Africa, evidence that biome-associated species in other groups may also have persisted where biomes

400 persisted, elsewhere showing range shifts as climatic conditions changed (Tolley *et al.*, 2014), suggests

401 that our results may be more general.

402 Our results increase concerns about the potential for future biodiversity losses resulting from biome

403 replacements.   Given projections that more than half Earth's land area may experience climatic changes

404 by 2100 sufficient to cause biome replacement (Williams *et al.*, 2007), we conclude that future biome

405 replacement resulting from anthropogenic climatic change is likely to result in substantial biodiversity losses

406 worldwide.   Avoiding such losses will require a combination of vigorous mitigation measures, so as to limit

407 the magnitude of climatic change as far as possible, and active conservation measures designed to sustain

408 species' populations and facilitate their spatial responses to changing conditions.

REFERENCES

Allouche, O., Tsoar, A. & Kadmon, R. (2006) Assessing the accuracy of species distribution models: prevalence, kappa and the true skill statistic (TSS). *Journal of Applied Ecology*, **43**, 1223-1232.

Allsopp, N., Colville, J.F. & Verboom, G.A. (eds) (2014) *Fynbos: Ecology, evolution and conservation of a megadiverse region*. Oxford University Press, Oxford.

Araújo, M.B., Nogués-Bravo, D., Diniz-Filho, J.A.F., Haywood, A.M., Valdes, P.J. & Rahbek, C. (2008) Quaternary climate changes explain diversity among reptiles and amphibians. *Ecography*, **31**, 8-15.

Barnola, J.M., Raynaud, D., Korotkevich, Y.S. & Lorius, C. (1987) Vostoc ice core provides 160,000-years record of atmospheric CO_2. *Nature*, **329**, 408-414.

Boelhouwers, J.C. & Meiklejohn, K.I. (2002) Quaternary periglacial and glacial geomorphology of southern Africa: review and synthesis. *South African Journal of Science*, **98**, 47-55.

Bond, G., Showers, W., Cheseby, M., Lotti, R., Almasi, P., de Menocal, P., Priore, P., Cullen, H., Hajdas, I. & Bonani, G. (1997) A pervasive millennial-scale cycle in North Atlantic Holocene and glacial climates. *Science*, **278**, 1257-1266.

Bond, W.J. & Midgley, G.F. (2012) Carbon dioxide and the uneasy interactions of trees and savannah grasses. *Philosophical Transactions of the Royal Society B-Biological Sciences*, **367**, 601-612.

Campos, P.F., Kristensen, T., Orlando, L., Sher, A., Kholodova, M.V., Gotherstrom, A., Hofreiter, M., Drucker, D.G., Kosintsev, P., Tikhonov, A., Baryshnikov, G.F., Willerslev, E. & Gilbert, M.T.P. (2010) Ancient DNA sequences point to a large loss of mitochondrial genetic diversity in the saiga antelope (*Saiga tatarica*) since the Pleistocene. *Molecular Ecology*, **19**, 4863-4875.

Chase, B.M. & Meadows, M.E. (2007) Late Quaternary dynamics of southern Africa's winter rainfall zone. *Earth-Science Reviews*, **84**, 103-138.

Cohen, J. (1960) A coefficient of agreement for nominal scales. *Educational and Psychological Measurements*, **20**, 37-46.

Colville, J.F., Potts, A.J., Bradshaw, P.L., Measey, G.J., Snijman, D., Picker, M.D., Bowie, R.C.K. & Manning., J.C. (2014) Floristic and faunal Cape biochoria: Do they exist? *Fynbos: Ecology, evolution and conservation of a megadiverse region* (ed. by N. Allsopp, J.F. Colville and G.A. Verboom), pp. 73-92. Oxford University Press, Oxford.

Dynesius, M. & Jansson, R. (2000) Evolutionary consequences of changes in species' geographical distributions driven by Milankovitch climate oscillations. *Proceedings of the National Academy of Sciences of the United States of America*, **97**, 9115-9120.

Ehlers, J. & Gibbard, P.L. (eds) (2004) *Quaternary glaciations: Extent and chronology (3 Vols.)*. Elsevier Science, Amsterdam.

Elenga, H., Peyron, O., Bonnefille, R., Jolly, D., Cheddadi, R., Guiot, J., Andrieu, V., Bottema, S., Buchet, G., de Beaulieu, J.L., Hamilton, A.C., Maley, J., Marchant, R., Perez-Obiol, R., Reille, M., Riollet, G., Scott, L., Straka, H., Taylor, D., Van Campo, E., Vincens, A., Laarif, F. & Jonson, H. (2000) Pollen-based biome reconstruction for southern Europe and Africa 18,000 yr BP. *Journal of Biogeography*, **27**, 621-634.

EPICA community members (2004) Eight glacial cycles from an Antarctic ice core. *Nature*, **429**, 623-628.

Etheridge, D.M., Steele, L.P., Langenfelds, R.L., Francey, R.J., Barnola, J.M. & Morgan, V.I. (1996) Natural and anthropogenic changes in atmospheric CO_2 over the last 1000 years from air in Antarctic ice and firn. *Journal of Geophysical Research-Atmospheres*, **101**, 4115-4128.

Gaston, K.J. (2000) Global patterns in biodiversity. *Nature*, **405**, 220-227.

Gordon, C., Cooper, C., Senior, C.A., Banks, H., Gregory, J.M., Johns, T.C., Mitchell, J.F.B. & Wood, R.A. (2000) The simulation of SST, sea ice extents and ocean heat transports in a version of the Hadley Centre coupled model without flux adjustments. *Climate Dynamics*, **16**, 147-168.

Graham, R.W. & Grimm, E.C. (1990) Effects of global climate change on the patterns of terrestrial biological communities. *Trends in Ecology and Evolution*, **5**, 289-292.

Harrison, J.A., Allan, D.G., Underhill, L.G., Herremans, M., Tree, A.J., Parker, V. & Brown, C.J. (eds) (1997) *The atlas of southern African birds*. BirdLife South Africa, Johannesburg.

Hewitt, G.M. (1996) Some genetic consequences of ice ages, and their role in divergence and speciation. *Biological Journal of the Linnean Society*, **58**, 247-276.

Hewitt, G.M. (2001) Speciation, hybrid zones and phylogeography - or seeing genes in space and time. *Molecular Ecology*, **10**, 537-549.

Hockey, P.A.R., Dean, W.R.J. & Ryan, P.G. (eds) (2005) *Roberts birds of southern Africa*, VIIth Edition. The Trustees of the John Voelcker Bird Book Fund, Cape Town.

Huntley, B. (1991) How plants respond to climate change: migration rates, individualism and the consequences for plant communities. *Annals of Botany*, **67**, 15-22.

474   Huntley, B. (1993) Species-richness in north-temperate zone forests. *Journal of Biogeography*, **20**, 163-
475   180.

476   Huntley, B. & Webb, T., III (1989) Migration: species' response to climatic variations caused by changes in
477   the earth's orbit. *Journal of Biogeography*, **16**, 5-19.

478   Huntley, B., Bartlein, P.J. & Prentice, I.C. (1989) Climatic control of the distribution and abundance of
479   beech (*Fagus* L.) in Europe and North America. *Journal of Biogeography*, **16**, 551-560.

480   Huntley, B., Midgley, G.F., Barnard, P. & Valdes, P.J. (2014) Sub-orbital climatic variability and centres of
481   biological diversity in the Cape region of southern Africa. *Journal of Biogeography*, **41**, 1338-1351.

482   Huntley, B., Altwegg, R., Barnard, P., Collingham, Y.C. & Hole, D.G. (2012) Modelling relationships
483   between species' spatial abundance patterns and climate. *Global Ecology and Biogeography*, **21**, 668-
484   681.

485   Huntley, B., Collingham, Y.C., Green, R.E., Hilton, G.M., Rahbek, C. & Willis, S.G. (2006) Potential impacts
486   of climatic change upon geographical distributions of birds. *Ibis*, **148**, 8-28.

487   Hutchinson, M.F. (1989) *A new objective method for spatial interpolation of meteorological variables from
488   irregular networks applied to the estimation of monthly mean solar radiation, temperature, precipitation
489   and windrun*. Technical Memo., 89/5. CSIRO Division of Water Resources, Canberra, Australia.

490   Indermühle, A., Stocker, T.F., Joos, F., Fischer, H., Smith, H.J., Wahlen, M., Deck, B., Mastroianni, D.,
491   Tschumi, J., Blunier, T., Meyer, R. & Stauffer, B. (1999) Holocene carbon-cycle dynamics based on
492   CO_2 trapped in ice at Taylor Dome, Antarctica. *Nature*, **398**, 121-126.

493   IOC, IHO & BODC (2003) Centenary Edition of the GEBCO Digital Atlas, published on CD-ROM on behalf
494   of the Intergovernmental Oceanographic Commission and the International Hydrographic Organization
495   as part of the General Bathymetric Chart of the Oceans. British Oceanographic Data Centre, Liverpool,
496   UK.

497   Jetz, W. & Rahbek, C. (2002) Geographic range size and determinants of avian species richness. *Science*,
498   **297**, 1548-1551.

499   Jetz, W., Rahbek, C. & Colwell, R.K. (2004) The coincidence of rarity and richness and the potential
500   signature of history in centres of endemism. *Ecology Letters*, **7**, 1180-1191.

501   Kim, J.H., Schneider, R.R., Mulitza, S. & Muller, P.J. (2003) Reconstruction of SE trade-wind intensity
502   based on sea-surface temperature gradients in the southeast Atlantic over the last 25 kyr. *Geophysical
503   Research Letters*, **30**

504 Laskar, J., Robutel, P., Joutel, F., Gastineau, M., Correia, A.C.M. & Levrard, B. (2004) A long-term

505   numerical solution for the insolation quantities of the Earth. *Astronomy & Astrophysics*, **428**, 261-285.

506 Linder, H.P. & Hardy, C.R. (2004) Evolution of the species-rich Cape flora. *Philosophical Transactions of*

507   *the Royal Society of London Series B-Biological Sciences*, **359**, 1623-1632.

508 MacPhee, R.D.E., Tikhonov, A.N., Mol, D. & Greenwood, A.D. (2005) Late Quaternary loss of genetic

509   diversity in muskox (*Ovibos*). *BMC Evolutionary Biology*, **5**, 1-13.

510 Marchant, R., Cleef, A., Harrison, S.P., Hooghiemstra, H., Markgraf, V., van Boxel, J., Ager, T., Almeida, L.,

511   Anderson, R., Baied, C., Behling, H., Berrio, J.C., Burbridge, R., Bjorck, S., Byrne, R., Bush, M.,

512   Duivenvoorden, J., Flenley, J., De Oliveira, P., van Geel, B., Graf, K., Gosling, W.D., Harbele, S., van

513   der Hammen, T., Hansen, B., Horn, S., Kuhry, P., Ledru, M.P., Mayle, F., Leyden, B., Lozano-Garcia,

514   S., Melief, A.M., Moreno, P., Moar, N.T., Prieto, A., van Reenen, G., Salgado-Labouriau, M., Schabitz,

515   F., Schreve-Brinkman, E.J. & Wille, M. (2009) Pollen-based biome reconstructions for Latin America at

516   0, 6000 and 18 000 radiocarbon years ago. *Climate of the Past*, **5**, 725-767.

517 Markgraf, V. (1993) Climatic history of Central and South America since 18,000 yr B.P.: Comparison of

518   pollen records and model simulations. *Global climates since the last glacial maximum* (ed. by H.E.

519   Wright, Jr., J.E. Kutzbach, T. Webb, Iii, W.F. Ruddiman, F.A. Street-Perrott and P.J. Bartlein), pp. 357-

520   385. University of Minnesota Press, 2037 University Ave. S. E., Minneapolis, Minnesota 55455, USA;

521   University of Minnesota Press, London, England.

522 Markgraf, V. & McGlone, M. (2005) Southern temperate ecosystem responses. *Climate change and*

523   *biodiversity.* (ed. by T.E. Lovejoy and L. Hannah), pp. 142-156. Yale University Press, New Haven &

524   London.

525 McGlone, M.S. (1988) Glacial and Holocene vegetation history: New Zealand. *Vegetation History* (ed. by B.

526   Huntley and T. Webb, Iii), pp. 557-599. Kluwer Academic Publishers, Dordrecht.

527 Meadows, M.E. & Baxter, A.J. (1999) Late Quaternary palaeoenvironments of the southwestern Cape,

528   South Africa: a regional synthesis. *Quaternary International*, **57-8**, 193-206.

529 Midgley, G.F., Reeves, G. & Klak, C. (2005) Late Tertiary and Quaternary climate change and centres of

530   endemism in the southern African flora. *Phylogeny and Conservation* (ed. by A. Purvis, J.L. Gittleman

531   and T. Brooks), pp. 230-242. Cambridge University Press, New York.

Mills, S.C., Grab, S.W., Rea, B.R., Carr, S.J. & Farrow, A. (2012) Shifting westerlies and precipitation patterns during the late Pleistocene in southern Africa determined using glacier reconstruction and mass balance modelling. *Quaternary Science Reviews*, **55**, 145-159.

Mucina, L. & Rutherford, M.C. (eds) (2006) *The Vegetation of South Africa, Lesotho and Swaziland*. South African National Biodiversity Institute, Pretoria.

New, M., Hulme, M. & Jones, P. (1999) Representing twentieth-century space–time climate variability. Part I: Development of a 1961–90 mean monthly terrestrial climatology. *Journal of Climate*, **12**, 829-856.

Partridge, T.C., Scott, L. & Hamilton, J.E. (1999) Synthetic reconstructions of southern African environments during the last glacial maximum (21-18 kyr) and the Holocene altithermal (8-6 kyr). *Quaternary International*, **57-8**, 207-214.

Petit, J.R., Jouzel, J., Raynaud, D., Barkov, N.I., Barnola, J.-M., Basile, I., Bender, M., Chappellaz, J., Davis, M., Delaygue, G., Delmotte, M., Kotlyakov, V.M., Legrand, M., Lipenkov, V.Y., Lorius, C., Pépin, L., Ritz, C., Saltzman, E. & Stievenard, M. (1999) Climate and atmospheric history of the past 420,000 years from the Vostok ice core, Antarctica. *Nature*, **399**, 429-436.

Polley, H.W., Johnson, H.B., Marino, B.D. & Mayeux, H.S. (1993) Increase in C3 plant water-use efficiency and biomass over glacial to present CO_2 concentrations. *Nature*, **361**, 61-64.

Rahbek, C. & Graves, G.R. (2001) Multiscale assessment of patterns of avian species richness. *Proceedings of the National Academy of Sciences of the United States of America*, **98**, 4534-4539.

Sandel, B., Arge, L., Dalsgaard, B., Davies, R.G., Gaston, K.J., Sutherland, W.J. & Svenning, J.C. (2011) The influence of late Quaternary climate-change velocity on species endemism. *Science*, **334**, 660-664.

Scheiter, S. & Higgins, S.I. (2009) Impacts of climate change on the vegetation of Africa: an adaptive dynamic vegetation modelling approach. *Global Change Biology*, **15**, 2224-2246.

Singarayer, J.S. & Valdes, P.J. (2010) High-latitude climate sensitivity to ice-sheet forcing over the last 120 kyr. *Quaternary Science Reviews*, **29**, 43-55.

Singarayer, J.S. & Burrough, S.L. (2015) Interhemispheric dynamics of the African rainbelt during the late Quaternary. *Quaternary Science Reviews*, **124**, 48-67.

Thomas, D.S.G., O'Connor, P.W., Bateman, M.D., Shaw, P.A., Stokes, S. & Nash, D.J. (2000) Dune activity as a record of late Quaternary aridity in the northern Kalahari: new evidence from northern Namibia interpreted in the context of regional arid and humid chronologies. *Palaeogeography Palaeoclimatology Palaeoecology*, **156**, 243-259.

562 Thuiller, W., Midgley, G.F., Rouget, M. & Cowling, R.M. (2006) Predicting patterns of plant species richness

563 in megadiverse South Africa. *Ecography*, **29**, 733-744.

564 Tolley, K.A., Bowie, R.C.K., Measey, G.J., Price, B.W. & Forest, F. (2014) The shifting landscape of genes

565 since the Pliocene: Terrestrial phylogeography in the Greater Cape Floristic Region. *Fynbos: Ecology,*

566 *evolution and conservation of a megadiverse region* (ed. by N. Allsopp, J.F. Colville and G.A.

567 Verboom), pp. 142-163. Oxford University Press, Oxford.

568 Voelker, G., Outlaw, R.K. & Bowie, R.C.K. (2010) Pliocene forest dynamics as a primary driver of African

569 bird speciation. *Global Ecology and Biogeography*, **19**, 111-121.

570 Williams, J.W., Jackson, S.T. & Kutzbach, J.E. (2007) Projected distributions of novel and disappearing

571 climates by 2100 AD. *Proceedings of the National Academy of Sciences of the United States of*

572 *America*, **104**, 5738-5742.

573 Wolff, E.W., Chappellaz, J., Blunier, T., Rasmussen, S.O. & Svensson, A. (2010) Millennial-scale variability

574 during the last glacial: The ice core record. *Quaternary Science Reviews*, **29**, 2828-2838.

575 **Supporting Information**

576 Additional Supporting Information may be found in the online version of this article:

577 **Appendix S1:   Supplementary tables and figures**

578 **Appendix S2:   Supplementary text**

579 **Appendix S3:   Supplementary tables and figures of results**

580 **Biosketch**

581 **Brian Huntley** is a palaeoecologist, ecologist and biogeographer with research interests in the interactions
582 between species, ecosystems and their changing environment. His work encompasses studies of the
583 palaeoecology and palaeoenvironments of the Quaternary, of present ecosystems and biogeographic
584 patterns, and of the potential impacts of anthropogenic global change on species and ecosystems. His
585 research has considered a range of taxonomic groups, from plants to extinct Quaternary mammals, and
586 various ecosystems, from Arctic tundra to fynbos. He has a particular interests in birds and climatic
587 change, and in the development of conservation strategies informed by research into how species and
588 ecosystems respond to environmental changes.

589 BH and GFM conceived the study.   PJV and JSS performed the palaeoclimate simulations.   BH carried
590 out the assessment of climatic variability, biome and species' modelling, analysis of results, preparation of
591 figures and drafting of the manuscript.   All authors commented upon and contributed to the final version of
592 the manuscript.

593 Editor: Jon Sadler

594 **TABLES**

595 **Table 1:   Species richness and climatic variability**

596 **Table 2:   Endemic species richness and biome stability**

Table 1: Species richness and climatic variability

Species group	Overall climatic difference			Climatic difference with respect to present climate		
	Maximum	Mean	S.D.	Maximum	Mean	S.D.
All species						
Overall	-0·006	0·017	-0·070	-0·016	**0·174**	-0·064
Residents	0·065	**0·110**	0·001	0·045	**0·274**	0·007
Mobile species	-0·057	-0·051	**-0·116**	-0·059	0·090	**-0·111**
Intra-African migrants	0·043	0·078	-0·024	0·025	**0·248**	-0·019
Widespread species	0·050	0·089	-0·015	0·031	**0·254**	-0·011
Endemic species						
Overall	**-0·263**	**-0·344**	**-0·247**	**-0·220**	**-0·395**	**-0·244**
Residents	**-0·143**	**-0·202**	**-0·164**	**-0·112**	**-0·153**	**-0·160**
Mobile species	**-0·279**	**-0·358**	**-0·252**	**-0·236**	**-0·436**	**-0·250**

Pearson product–moment correlation coefficients between present simulated avian species richness and six measures of climatic variability over the past 140 kyr for 0·5° grid cells in southern Africa ($n = 1461$, bold entries indicate values for which $p < 0.0005$). Climatic variability is expressed as the maximum, mean or standard deviation of standardised Euclidean distances between climatic conditions calculated either for all time slices, including the present, relative to one another (overall climatic difference), or for all palaeoclimatic time slices relative to the present. High variability of climate thus corresponds to high Euclidean distance values, whereas a high degree of stability of climate is indicated by low Euclidean Distance values. Correlation coefficients are shown for all species, for all species categorised according to seasonal movements, for widespread (i.e. non-endemic) species, for all endemics and for endemics categorised according to seasonal movements (note that Intra-African migrants cannot by definition be endemic or near-endemic to southern Africa). Negative correlations indicate high species richness associated with low climatic variability (i.e. low Euclidean distance values, and hence high climatic stability) and *vice versa*.

Table 2:   Endemic species richness and biome stability

Biome	All of southern Africa			South of 22°S		
	Frequency of dominance	Mean percentage occupied	Frequency of occurrence	Frequency of dominance	Mean percentage occupied	Frequency of occurrence
Desert	0·474	0·673	0·725	0·469	0·599	0·645
Karoo	0·743	0·751	0·770	0·638	0·646	0·674
Fynbos	0·326	0·180	0·213	0·575	0·615	0·482
Albany Thicket	0·318	0·471	0·424	0·342	0·501	0·492
Grassland	0·722	0·762	0·711	0·720	0·799	0·763
Savanna	-0·247	-0·367	-0·293	*0·029*	*0·024*	*0·071*
Forest	–	0·299	0·308	–	0·497	0·698

612 Pearson product–moment correlation coefficients between present simulated avian species richness of

613 endemics using each of seven regional biomes in southern Africa as their principal habitat and three

614 measures of the simulated stability of those biomes over the past 140 kyr for 0·5° grid cells (entries in italics

615 are values for which $p > 0.025$; $p < 0.0005$ for all other values).   Correlations are presented both for the

616 entire study region ($n = 1461$) and for the area south of 22°S that corresponds approximately to the region

617 from which the data used to construct models relating biome extents to climate were available ($n = 823$).

618 The three measures of biome stability are: the frequency, across all time slices, with which the biome

619 dominates the grid cell (i.e. is simulated to extend over a greater percentage of the land area of the grid cell

620 than does any other biome);   the mean extent of the biome in the grid cell, across all time slices,

621 expressed as the percentage of the area of land in the grid cell simulated to be occupied by the biome;

622 and the frequency, across all time slices, with which the biome is simulated to be present in the grid cell.

623 Positive correlations indicate high species richness associated with high stability of the associated biome.

FIGURES

625 **Figure 1:   Map of Southern Africa**
626 The overall extent of the map corresponds to the overall study area for which climatic variability was
627 assessed and for which projections were made using the response surface models for biomes and bird
628 species.   Distribution data used to fit the models for bird species extended across South Africa, Lesotho,
629 Swaziland, Namibia, Botswana and Zimbabwe.   Biome extent data used to fit the models for biomes
630 extended over the area south of the red boundary line, i.e. South Africa, Lesotho and Swaziland.   Country
631 names are in black upright text and South African province names in red text;   geographical features
632 mentioned in the text are indicated by italic black text.   Topography is shown using the GEBCO 1′
633 resolution global altitudinal and bathymetric grid (IOC *et al.*, 2003).

634 **Figure 2:   Climatic variability in southern Africa since 140 ka**
635 Maximum (a & d), mean (b & e) and standard deviation (c & f) of Euclidean Distances between present
636 climate and 78 palaeoclimate time slices (a–c), and of all possible pairwise Euclidean Distances (d–f)
637 between the 79 climates, for each 0·5° grid cell.   Deep orange indicates low climatic variability (i.e.
638 minimum Euclidean Distances) whereas deep blue indicates high climatic variability (i.e. maximum
639 Euclidean Distances).   Mapping of Euclidean Distance values to the colour scale in each case was
640 designed to provide the clearest representation of the spatial pattern of climatic variability.

641 **Figure 3:   Simulated biome distributions for southern Africa**
642 Maps show the biome simulated to dominate each 0·5° grid cell for a set of time slices selected to show the
643 extreme contrasts corresponding to time-slice pairs most frequently giving maximum climatic differences,
644 as well as to illustrate responses to both orbital and sub-orbital forcing.   The 22, 46, 70, 92, 116 and
645 138 ka time slices correspond approximately to austral summer (December–January) insolation maxima at
646 30°S, whilst 11, 32, 60, 82, 104 and 124 ka correspond approximately to austral summer insolation minima
647 at 30°S.   The H0, H1, H2, H5 and H6 simulations of Heinrich Events, at close to 13, 17, 24, 46 and 60 ka
648 respectively, reflect maximal millennial climatic contrasts relative to conditions simulated using only orbital
649 and other 'slow' forcing factors.

650 **Figure 4:   Relative extent of each biome in southern Africa over the past 140 kyr**
651 Simulated extent of each biome for each palaeoclimate scenario, relative to its extent for 1961–90, plotted
652 against age.   Also shown are the austral summer (December–January) insolation at 30°S, computed
653 following Laskar *et al.* (2004), and atmospheric CO_2 concentration, derived as a composite from the Law
654 Dome (Etheridge *et al.*, 1996, 0-0.940 ka), Taylor Dome (Indermühle *et al.*, 1999, 1.020-11.103 ka) and
655 Vostok (Barnola *et al.*, 1987, 12.930-140.430 ka) Antarctic Ice Cores.   Grey lines indicate Heinrich Events
656 0 – 6.

657 **Figure 5:   Frequency with which biomes were simulated to dominate grid cells**
658 Shading indicates for how many of the 79 time slices examined, including the present, climatic conditions in
659 each grid cell result in simulated dominance of a given biome.   (IOCB = Indian Ocean Coastal Belt.
660 Forest was not simulated as the dominant biome in any grid cell for any time slice.)
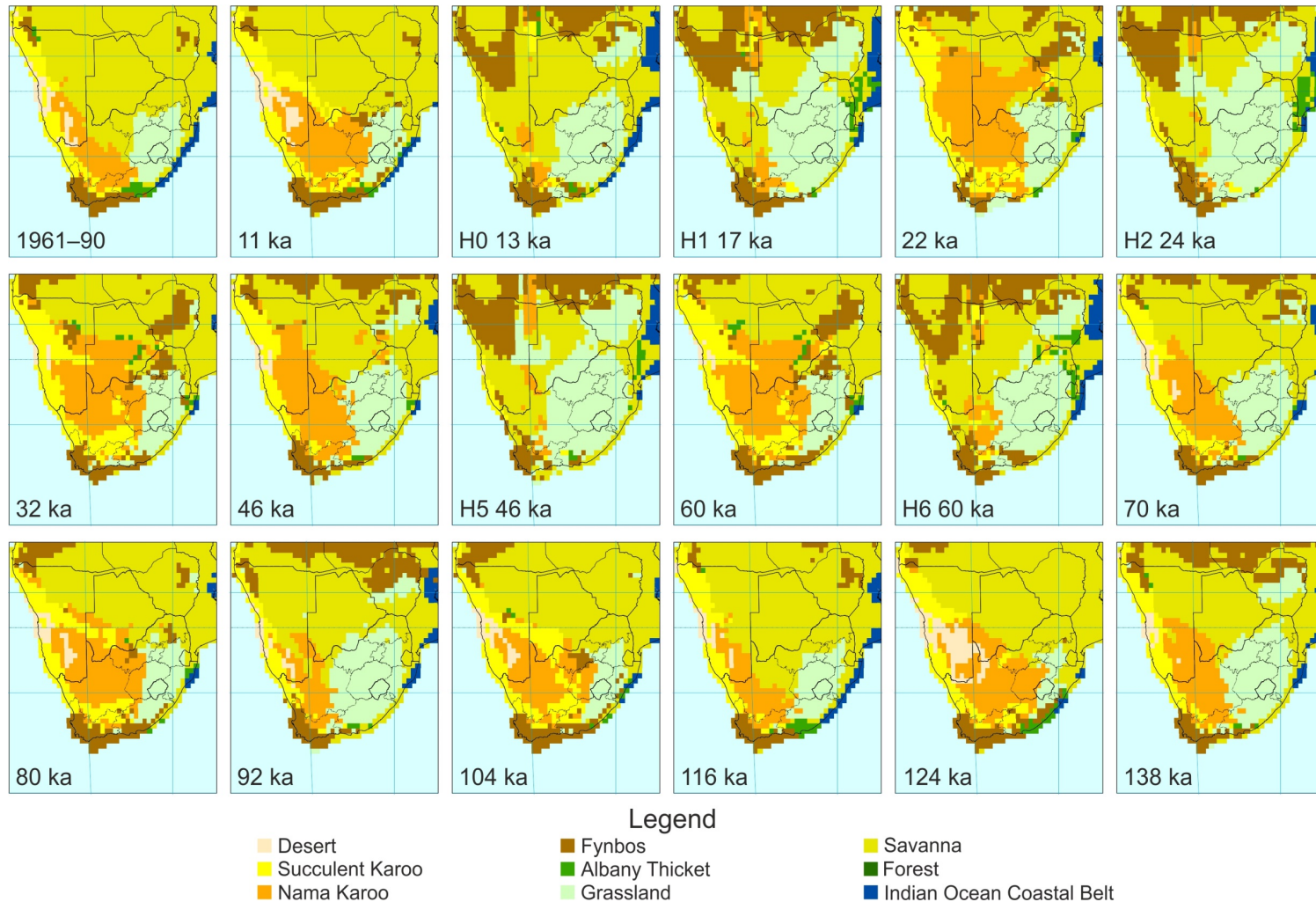
Figure 1:   Map of Southern Africa

The overall extent of the map corresponds to the overall study area for which climatic variability was assessed and for which projections were made using the response surface models for biomes and bird species.   Distribution data used to fit the models for bird species extended across South Africa, Lesotho, Swaziland, Namibia, Botswana and Zimbabwe.   Biome extent data used to fit the models for biomes extended over the area south of the red boundary line, i.e. South Africa, Lesotho and Swaziland.   Country names are in black upright text and South African province names in red text;   geographical features mentioned in the text are indicated by italic black text.   Topography is shown using the GEBCO 1′ resolution global altitudinal and bathymetric grid (IOC *et al.*, 2003).
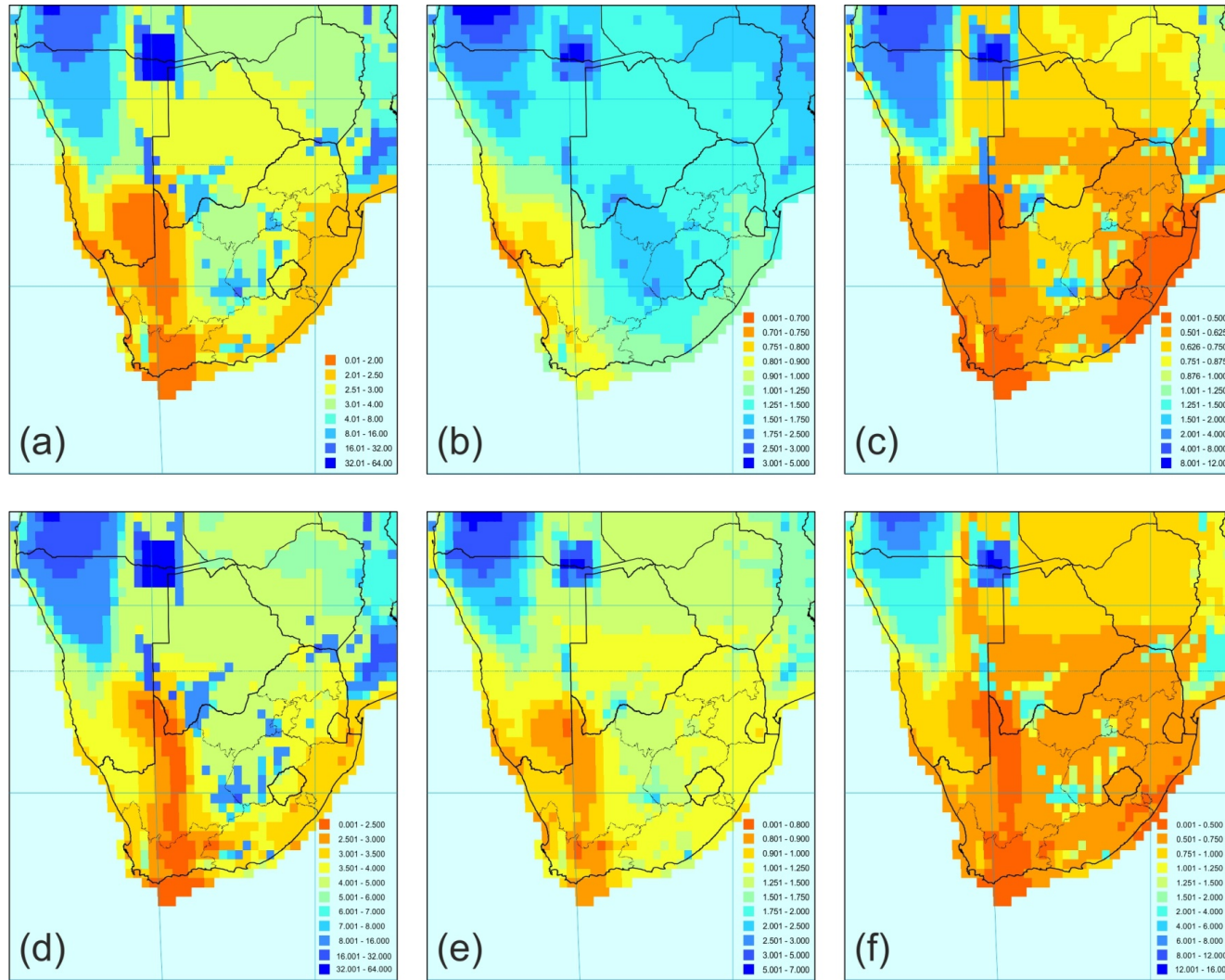
**Figure 2: Climatic variability in southern Africa since 140 ka**

Maximum (a & d), mean (b & e) and standard deviation (c & f) of Euclidean Distances between present climate and 78 palaeoclimate time slices (a–c), and of all possible pairwise Euclidean Distances (d–f) between the 79 climates, for each 0·5° grid cell. Deep orange indicates low climatic variability (i.e. minimum Euclidean Distances) whereas deep blue indicates high climatic variability (i.e. maximum Euclidean Distances). Mapping of Euclidean Distance values to the colour scale in each case was designed to provide the clearest representation of the spatial pattern of climatic variability.

30

Legend

Desert	Fynbos	Savanna
Succulent Karoo	Albany Thicket	Forest
Nama Karoo	Grassland	Indian Ocean Coastal Belt

**Figure 3: Simulated biome distributions for southern Africa**

Maps show the biome simulated to dominate each 0·5° grid cell for a set of time slices selected to show the extreme contrasts corresponding to time-slice pairs most frequently giving maximum climatic differences, as well as to illustrate responses to both orbital and sub-orbital forcing. The 22, 46, 70, 92, 116 and 138 ka time slices correspond approximately to austral summer (December–January) insolation maxima at 30°S, whilst 11, 32, 60, 82, 104 and 124 ka correspond approximately to austral summer insolation minima at 30°S. The H0, H1, H2, H5 and H6 simulations of Heinrich Events, at close to 13, 17, 24, 46 and 60 ka respectively, reflect maximal millennial climatic contrasts relative to conditions simulated using only orbital and other 'slow' forcing factors.
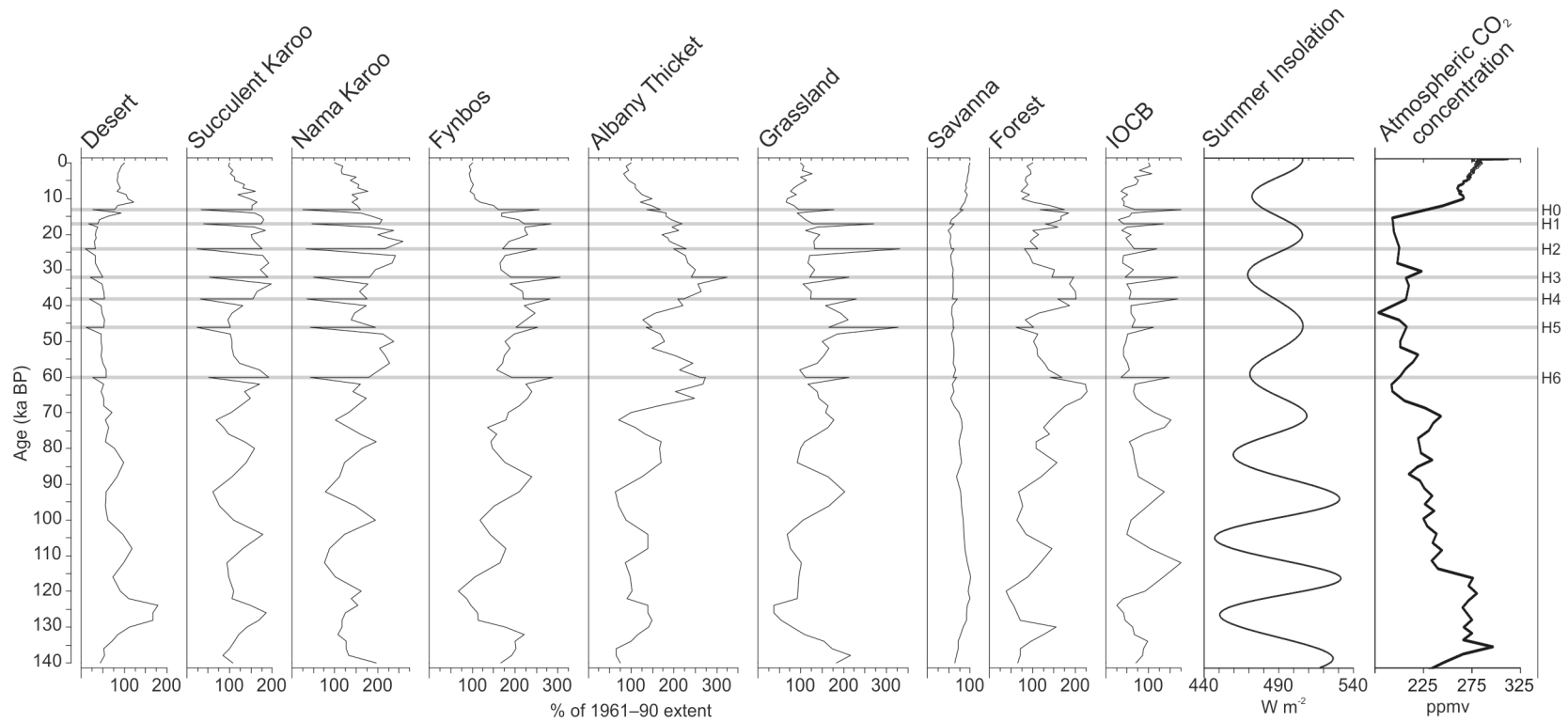
684

685 **Figure 4: Relative extent of each biome in southern Africa over the past 140 kyr**

686 Simulated extent of each biome for each palaeoclimate scenario, relative to its extent for 1961–90, plotted against age. Also shown are the austral summer

687 (December–January) insolation at 30°S, computed following Laskar *et al.* (2004), and atmospheric CO_2 concentration, derived as a composite from the Law

688 Dome (Etheridge *et al.*, 1996, 0-0.940 ka), Taylor Dome (Indermühle *et al.*, 1999, 1.020-11.103 ka) and Vostok (Barnola *et al.*, 1987, 12.930-140.430 ka)

689 Antarctic Ice Cores. Grey lines indicate Heinrich Events 0 – 6.
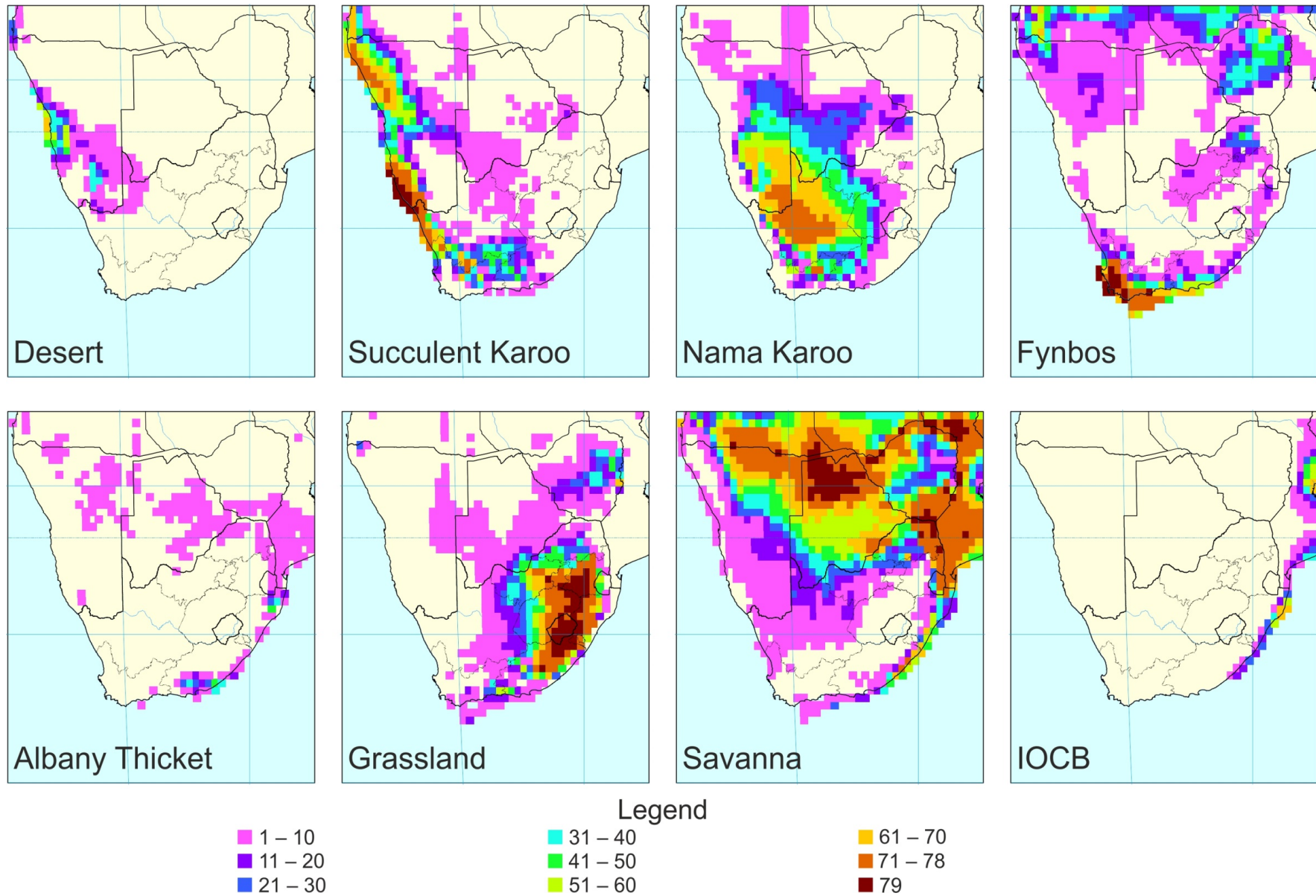
Figure 5: Frequency with which biomes were simulated to dominate grid cells

Shading indicates for how many of the 79 time slices examined, including the present, climatic conditions in each grid cell result in simulated dominance of a given biome. (IOCB = Indian Ocean Coastal Belt. Forest was not simulated as the dominant biome in any grid cell for any time slice.)